An Experimental Analysis of Embankment on Stone Columns

Dr. Mohammed Y.Fattah
Professor
Building and Construction Department
University of Technology
E-mail:myf_1968@yahoo.com

Dr. Bushra S.Zabar
Assistant Professor
College of Engineering
University of Baghdad
E-mail albusoda@yahoo.com

Hanan A. Hassan
Instructor
College of Engineering
University of Al-Mustansiriya
E-mail: ghassan_hanan@yahoo.com

ABSTRACT

When embankment is constructed on very soft soil, special construction methods are adopted. One of the techniques is a piled embankment. Piled (stone columns) embankments provide an economic and effective solution to the problem of constructing embankments over soft soils. This method can reduce settlements, construction time and cost. Stone columns provide an effective improvement method for soft soils under light structures such as rail or road embankments. The present work investigates the behavior of the embankment models resting on soft soil reinforced with stone columns. Model tests were performed with different spacing distances between stone columns and two lengths to diameter ratios of the stone columns, in addition to different embankment heights. A total number of 21 model tests were carried out on a soil with undrianed shear strength ≈ 10 kPa. The models consist of stone columns embankment at spacing to diameter ratio equal to 2.5, 3 and 4. Three embankment heights; 200 mm, 250 mm and 300 mm were conducted. Three earth pressure cells were used to measure directly the vertical effective stress on column at the top of the middle stone column under the center line of embankment and on the edge stone column for all models while the third cell was placed at the base of embankment between two columns to measure the vertical effective stress in reinforced soft soil directly. The embankment models constructed on soft clay treated with ordinary stone columns at spacing ratio equal 2.5 revealed maximum bearing improvement ratio equals (1.21, 1.44 and 1.7) for 200 mm, 250 mm and 300 embankment heights, respectively and maximum settlement improvement ratio equals (0.78, 0.67 and 0.56) for 200 mm, 250 mm and 300 embankment heights, respectively.

Keywords: stone columns, soft clay, embankment, laboratory models.

تحليل عملي لسدة ترابيه مستندة على أعمدة حجرية

أ.د. محمد يوسف فتاح
قسم البناء والانشاءت
الجامعة التكنولوجية

أ.م.د. بشرى سهيل زبار
قسم الهندسة المدنية
كلية الهندسة/ جامعة بغداد

م. حنان عدنان حسن
قسم الطرق والنقل
كلية الهندسة/ الجامعة المستنصيرية

الخلاصة

ان انشاء سدة على تربة طينية رخوة يحتاج الى طرق خاصة. احدى هذه الطرق هو استخدام الركائز الحجرية تحت السدة. حيث توفر هذه الطريقة حلاً اقتصادياً وفعالاً لمشاكل انشاء السدة فوق تربة طينية رخوة. تقلل هذه الطريقة الهبوط ووقت وكلفة الانشاء, تعتبر الاعمدة الحجرية طريقة تحسين فعالة تحت الاحمال الخفيفة مثل احمال السدة لسكة قطار او الطريق. اجريت هذه الدراسة على مجموعة موديلات بلغت 42 موديل تضمنت تربة طينية رخوة ذات مقاومة قص غير مبزول ≈ 10 كيلوباسكال مع اعمدة

حجرية عادية تم ترتيبها بنمط مربع الشكل مع مسافات مركزية بين عمود واخر تساوي 4 ,3 ,2.5 من قطر العمود كما تم تغيير ارتفاع السدة حيث بلغ 200ملم, 250ملم و300 ملم. وجد من دراسة موديلات لسدة مستندة على تربة طينية رخوة مثبته بأعمدة حجرية ، إن الاعمدة الحجرية المرتبه بمسافة مركزية (2.5) أظهرت أعلى نسبة تحسن في قابلية تحمل التربة حيث بلغت (1.21, 1.44و1.7) لسدة بارتفاع 200ملم, 250ملم و300 ملم. وأقل نسبة تحسن في نسبة الهبوط وبلغت (0.78, 0.67 و 0.56) لسدة بارتفاع 200ملم, 250ملم و300 ملم.

1. INTRODUCTION

The stone column method is the most effective soft soil improvement with undrained shear strength cu > 15 kN/m^2. Stone columns have higher drainage ability and stiffness than sand drains. Therefore, ground reinforcement by stone columns solves the problems of the soft soil by providing advantage of reduced settlement and accelerates consolidation process. Another advantage of this method is the simplicity of its construction. In extremely soft soil conditions, (c_u < 15 kN/m2), lateral support can be problematic for stone columns , **Kempfert, 2003.**

Stone columns provide the primary functions of reinforcement and drainage by improving the strength and deformation properties of the soft soil. Stone columns increase the unit weight of soil (due to densification of surrounding soil during construction), dissipate quickly the excess pore pressures generated and act as strong and stiff elements and carry higher shear stresses , M**adhav et. al., 1994, Yoo, 2010. Juran and Guermazi , 1988.** performed a series of special modified triaxial tests on soil reinforced with stone columns to study the effect of area replacement ratio (a_r) on the settlement reduction ratio. The results showed that the increase of replacement ratio from 0.04 to 0.16 results in a significant increase of the resistance of reinforced soil to the applied vertical load and reduce the settlement reduction ratio. **Rao et al. , 1997.** conducted a series of tests on stone columns installed in remolded soft clay with different soil consistencies (I_C) to study the effect of many parameters such as length to diameter of stone column, effect of the placement moisture content of the surrounding soil, the influence of spacing and the number of columns within the group on the ultimate bearing capacity. The study showed that the most effective length to diameter ratio was found to be ranged from 5 to 10. The consistency of soil (Ic = L.L-wn/PI) is one of the main factors that affect the load carrying capacity of the stone columns and controls the bulb formation.

Al- Shaikhly , 2000. carried out laboratory model tests to investigate the effect of grain size of backfill material, effect of length of stone columns and effect of area replacement ratio. The optimal size of backfill material for achieving the maximum value of improvement ranged from (11-14) % of the column diameter. For all types of the backfill material, the bearing ratio increased with increasing both the area ratio (a_r) and the length to diameter of the columns ratio (L/d).

Al-Qayssi , 2001. conducted model tests to improve the behavior of stone columns by using different patterns of reinforcement consisting of two and three discs connected to a central shaft. Influence of spacing between stone columns, effect of footing shape, effect of area replacement ratio and number of stone columns on ultimate bearing capacity was studied. The circular footing demonstrated a higher bearing ratio at failure followed by the square then by the rectangular model footings. The bearing ratio increased with increasing spacing from 2d, 2.5d and 3d c/c for all the three shapes of model footings. The area replacement ratio showed an insignificant influence on the efficiencies of the single stone column. Increasing number of stone columns caused a delay in the development of the bulging shape and hence improves the granular behavior. The bearing ratios for two and three discs giving an increase of 12% and 40% respectively over the single unreinforced stone columns.

Al-Waily , 2008. and Fattah et al. 2011. conducted a testing program to study the influence of stone column number (single, two, three, and four stone columns) , L/d ratio and undrained shear strength of bed soil on the stress concentration ratio and the bearing improvement ratio ($q_{treared}/q_{untreated}$) of stone columns. The experimental tests showed that the stone columns with L/d=8 provided a stress concentration ratio n of 1.4, 2.4, 2.7, and 3.1 for the soil having a shear strength cu=6 kPa, treated with single, two, three, and four columns, respectively. The values of n were decreased to 1.2, 2.2, 2.5, and 2.8 when the L/d=6. The values of n increase when the shear strength of the treated soil was increased to 9 and 12 kPa. The value of the bearing improvement ratio decreases with increasing the shear strength of the treated soil.

2. EXPERIMENTAL WORK

2.1 Soil Used

A brown clayey silt soil was brought from a depth of 5 m from the site of a bridge in the sport city within Al-Basrah government. The soil was subjected to routine laboratory tests to determine its properties, these tests include: grain size distribution (sieve analysis and hydrometer tests) according ASTM D422 specifications, Atterberg limits (liquid and plastic limits) according to ASTM D4318 and specific gravity according to ASTM D854 specifications. The results show that the soil consists of 6% sand, 46% clay and 48% silt as shown in **Fig. 1**. The soil is classified according to the Unified Soil Classification System USCS as (CL). **Table 1** shows the physical and chemical properties of the soil used.

2.2 Crushed Stone

The crushed stone, used as a backfill material was obtained from a private mosaic factory. The size of the crushed stone was chosen in accordance with the guidelines suggested by **Al-Shaikhly 2000,** where the particle size is about 1/7 to 1/9 of the diameter of stone columns. The particle size distribution is shown in **Fig. 2**, the particle sizes range between 2 to14 mm and found to have Ø value of 41.5º from direct shear test at a dry unit weight of 14.4 kN/m^3 corresponding to a relative density of 55%. The stone is uniform as its uniformity coefficient is less than 4 and considered as poorly graded. The physical properties are presented in **Table 2**.

2.3 Sub-base (Embankment Fill Material)

The granular sub-base was brought from Al-Nibaee quarry, north of Baghdad. The sub-base is commonly used as a fill material for embankment construction. **Fig. 3** shows the grain size distribution of sub-base according to (B.S.1377:1990, Test 7B). The physical and chemical properties of the sub-base used are shown in **Table 3**. The sub-base is classified as class (B) according to the **Iraqi SORB ,2003.** and as (GW) according to USCS.

3. MODEL DESIGN AND MANUFACTURING

To study the behavior of soft clay reinforced by ordinary stone columns underneath embankment; an experimental setup with an approximate scale of 1/20 to 1/30 of the prototype was designed and manufactured to achieve this goal. The setup consists of: steel container, loading frame, hydraulic system, load cell with load indicator, earth pressure cell, piezometer, strain gauge with strain indicator, footing model, dial gauges and data acquisition.

3.1 The Test Setup

***Steel container*:** A movable steel container was constructed to host the bed of soil and all accessories. The internal dimensions are 1500 mm length, 800 mm width and 1000 mm depth. The container was made of steel plates 6 mm in thickness braced externally by angles at their corners, edges and each side. The front side was made from tough glass. The container was provided with four wheels that allow it to move freely, the container is sufficiently rigid and exhibited no lateral deformation during preparation of soil and during the test. **Plate 1** shows details of the container.

Loading frame and axial loading system: The steel frame consists of two columns and a beam, each column is fixed at bottom by casting in a concrete slab. The axial pressure is applied through a hydraulic system which consists of three hydraulic jacks; one in the middle and the others on sides, used to apply the load on the embankment model, the location of the hydraulic jack is shown in **Plate 1**. The maximum stress that can be applied on a model footing (250 mm ×500 mm) reaches about 400 kPa. The pressure is measured by a load cell 50 kN in capacity connected to the digital load indicator as shown in **Plate 2**.

Earth pressure cell and readout: Earth pressure cells provide a direct means of measuring total pressure in or on bridge abutments, diaphragm walls, fills and embankments, retaining walls surfaces, sheet piling, slurry walls and tunnel lining. They may also be used to measure earth bearing pressure on foundation slabs and footings and at the tips of piles. **Plate 3** shows the earth pressure cell model 4800 manufactured by GEOKON company in U.S.A which is used in this study. Earth pressure cells are constructed from two thin stainless steel plates welded together around their periphery and separated by a narrow gap filled with hydraulic fluid. A length of stainless steel tubing connects the fluid filled cavity to a pressure transducer that converts the fluid pressure into an electrical signal transmitted by cable to the readout. They can be positioned in the fill at different orientations so that soil pressure can be measured in two or three directions. The vibrating wire readout box model GK404 manufactured by GEOKON company in U.S.A, used with earth pressure cell and piezometer, is portable, low-power, hand-held that is capable of running for more than 20 hours continuously. It is designed for the readout all GEOKON vibrating wire gages and transducers. **Plate 4** shows the readout device. The model GK404 provides 6 excitation positions (A-F) with display resolution of 0.1 digits. It is displaying the reading of one connector so that a suitable selector was manufactured to read all the instruments at the same time.

3.2 Preparation of Model Tests

3.2.1 Preparation of soil

Prior to the preparation of the soil bed in the container, the variation of shear strength of the clayey soil versus time after mixing at different liquidity indices should be obtained. Therefore; six samples with different liquidity indices were prepared individually; each sample was placed in five layers inside a CBR mould. Each layer was tamped gently with a special hammer to extract any entrapped air. The samples were then covered with polythen sheet and left for a period of eight days. Each day, the undrained shear strength was measured by a portable vane shear device, **Plate 5**. These tests provide the time required for the remolded soil to regain strength after a rest period following the mixing process, **Fig. 4**. The shear strength of soil decreases with the value of liquidity index and the influence of time decreases with liquidity index, **Fig. 5** shows the variation of shear strength of soil with liquidity indices after 96 hour curing.

According to the results obtained from **Fig. 5**, the soil was prepared in the manufactured container at undrained shear strength cu of 10 kPa and liquidity index of (0.48) corresponding to water content

of (34.5%). To perform soil preparation, 660 kg of air dried soil was divided into 30 kg groups; each group was mixed separately with enough quantity of water to get the desired consistency. The mixing operation was conducted using a large mixer manufactured for this purpose till completing the whole quantity. After thorough mixing, the wet soil was kept inside tightened polythen bags for a period of one day to get uniform moisture content. After that, the soil was placed in a steel container (1500×800×1000) mm in eleven layers; each layer was leveled gently using a wooden tamper of dimensions (50×100) mm. This process continues for the eleven layers till reaching a thickness of 560 mm of soil in the steel container. After completing the final layer, the top surface was scraped and leveled to get, as near as possible, a flat surface, then covered with polythen sheet to prevent any loss of moisture as shown in **Plate 6**. A wooden board of area similar to that of the soil surface area (1500× 800) mm was placed on the soil bed. The prepared soil was left for a period of four days to regain its strength reaching (10 kPa) as was suggested by , **Fattah et al. 2011.**

3.2.2 Installation of the stone columns

The position of the stone columns to be placed correctly in their proper locations was marked using a special frame manufactured according to the proposed configuration patterns of stone columns. A hollow steel pipe with external diameter of 70 mm coated with petroleum jelly was pushed down the bed to the specific depth (560 mm in fully penetrated stone column with L/d=8 and 350 mm for partially penetrated stone column with L/d=5) with the aid of the loading system. **Plate 7** shows process of the installation of the stone column. To remove the soil inside the casing, a hand auger, manufactured for this purpose was used. After that, the casing was removed carefully. The stones were carefully charged into the hole in ten layers and compacted at relative density of 55% using 50 mm diameter rod to achieve a dry unit weight of 14.4 kN/m^3 by a tamping rod. Spacing between stone columns for each configuration pattern is shown in **Plate 8**.

3.2.3 Installation of embankment fills

The construction of the embankment fill was started after installation of ordinary stone columns. A predetermined weight of sub-base was mixed with water by a mixer at optimum moisture content of 6.3%, this weight of sub-base is sufficient to create a uniform layer 50 mm thick. Each layer was compacted gently by a wooden tamper of size 75×75 mm to attain a placement maximum dry unit weight of 21.84 kN/m^3 until the desired embankment depth is obtained. Then the top layer was leveled using a piece of plywood. The final upper width of the embankment is 300 mm. **Plate 9** shows the process of preparation of the embankment.

3.2.4 Model testing procedure

The model tests were carried out on natural soil and soil improved with stone columns. The load cell and load readout used in testing program were calibrated by applying different known static loads and measuring values through the load cell before using. A footing (250 mm×600 mm) in dimensions was placed in position on the surface of the embankment model so that the center of the footing coincides with the center of the load cell and hydraulic jack. Two dial gauges with accuracy of (0.01 mm/division) were fixed in position to measure the settlements of plate and one dial gauge was placed in the toe of embankment to measure the soil heave as shown in **Plate 10**. Loads were then applied through a hydraulic jack in the form of load increments and measured by the load cell and recorded by load readout. During each load increment, the readings of the three dial gauges were recorded. The dial gauge readings were recorded at the end of the period of each load increment. Each load increment was left for (5 minutes) or till the rate of settlement became constant. **Plate 11** presents the tested models after completion of the tests.

4. PRESENTATION AND DISCUSSION OF TEST RESULTS

The investigation focuses on influence of parameters like, spacing of stone columns, length of stone column and height of embankment on overall behavior of soft soil treated by stone columns. The analysis of results of all model tests regarding the applied stress and the corresponding settlement is illustrated in terms of (q/c_u) vs (S/B). The (q/c_u) represents the ratio of applied stress to undrained shear strength of the soft clay, denoted as "bearing ratio" and (S/B) represents the corresponding vertical settlement as a percent of the model footing width, denoted as "settlement ratio". To obtain the degree of improvement achieved by each improvement technique, the results are plotted in the form of $(q/c_u)_t$ /($q/c_u)_{unt}$ denoted as "bearing improvement ratio", where $(q/c_u)_t$ is improved bearing ratio and $(q/c_u)_{unt}$ is unimproved bearing ratio.

The improvement in settlement achieved by the model tests is presented in the form of (S_t/S_{unt}) "settlement of treated soil to settlement of untreated soil at the same applied stress" denoted as "settlement improvement ratio", plotted against the bearing ratio (q/c_u).

4.1 Definition of Failure

The failure point is defined when the settlement reaches 36% of the diameter of the stone column or 10% of the width of the model footing. This definition is compatible with **Terzaghi,1947**, **Hughes and Withers,1974, Al-Mosawe et al., 1985 , and Fattah et al. 2011.**

4.1.1 Model tests on untreated embankment

Three model tests were conducted on beds of untreated soil with undrained shear strengths of 10 kPa at different embankment heights (200 mm, 250 mm and 300 mm). These tests are considered as reference to obtain the degree of improvement gained after introducing any other type of improvement technique.

Fig. 6 shows the relationship between the pressure (q) and the surface settlement of embankment (S) for model test, the figure illustrates that the mode of failure of model test is close to local shear pattern, due to the rapid rate of deformation. In this test, the footing model is resting on compacted layer (sub-base) of width relatively ≈ the footing width. The ultimate bearing capacity obtained is 35 kPa, 33 kPa and 30 kPa for the model tests of embankment height 200 mm, 250 mm and 300 mm respectively based on the failure criterion of (10% of footing width). **Fig. 7** shows the bearing ratio plotted against settlement ratio. The figure demonstrates that the soil bed underneath the 200 mm embankment height exhibited higher bearing ratio. The bearing ratios at failure (q/c_u) for the embankment- soft soil model are 3.5, 3.3 and 3.0 corresponding to the settlement ratio of 10% of the footing width and for embankment heights 200, 250 and 300 mm respectively. The results demonstrate a substantial decrease in bearing ratio with increasing thickness of embankment; this is due to the increase in the settlement induced by the load from embankment and applied stress.

4.1.2 Model tests of embankment treated with stone columns

Bearing capacity: This series consists of eighteen model tests performed with 200, 250 and 300 mm embankment overlying soft clay and immediately underneath the model footing. **Figs. 8** to **10** show the relationship between pressure and embankment surface settlement. The results show increase in the surface settlement with increasing spacing of columns for applied pressure. The maximum bearing capacity of soil was observed for soft soil improved with stone columns at (s/d =2.5) and the minimum bearing capacity was for soft soil improved with stone columns at (s/d =4). This may be

explained by the reduction in area ratio from 12.53 % to 4.89 %. Similar conclusions were obtained by **Han and Gabr ,2002, and Murugesan and Rajagopal ,2006.** In addition, it can be noticed that a higher embankment height resting on stone columns would result in a higher bearing pressure. Heave at the end of embankment versus horizontal distance from center line of embankment for different spacing and two L/d ratios are shown in **Figs. 11 to 14**.

Bearing ratio verses settlement ratio: The variation of bearing ratio (q/c_u) versus settlement ratio (S/B) is shown in **Figs. 15 to 17**. The results show the effect of ordinary stone columns on bearing ratio of soil. The spacing ratio (s/d =2.5), demonstrates higher bearing ratio at failure, as compared with spacing ratio (s/d = 4). Such behavior may be explained due to the confinement effect provided by the surrounding soil and the adjacent stone columns. As spacing ratio decreased, the confinement stress provided by the surrounding soil increases. Since the stone columns are stiffer than the surrounding soil, the stress concentration on the stone columns increases with decreasing the spacing of stone and embankment height due to soil arching. The values of bearing ratio at failure are summarized in **Table 4**. The present results are in agreement with the results obtanied by **Juran and Guermazi ,1988, Craig and Al-Kahafaji ,1997, Rahil ,2007, Al-Waily ,2008 and Fattah et al. 2011.**

Bearing improvement ratio verses settlement ratio: To evaluate the amount of improvement achieved by the ordinary stone column for different spacings over untreated soil, the bearing improvement ratio (q_t/q_{unt}) versus settlement ratio S/B% is presented in **Figs. 18 to 20**. Peak values of improvement ratio are observed at nearly S/B about 2% to 4% then drops down and decreased with increasing settlement ratio. This behavior is attributed to the load transfer mechanism, the stress is transferred to the stone columns expressing these peak values then it is gradually transferred to the surrounding soil implied by the drop in the improvement ratio. Also, it can be noticed that the stone columns with spacing ratio (s/d= 2.5) has higher improvement ratio for different embankment heights, which is attributed to the increase in area replacement. **Table 5** summarizes the values of bearing improvement ratio at failure.

Settlement improvement ratio versus bearing ratio: Variation of settlement improvement ratio (S_t/S_{unt}) versus bearing ratio (q/c_u) for different column spacings and embankment heights is shown in **Figs. 21 to 23**.The results imply a decrease in settlement improvement ratio as the bearing ratio increases until reaching (q/c_u) equals 1.48 to 2.8, then a gradual increase in settlement improvement ratio takes place, the decrease in settlement improvement ratio shows the level of improvement. This behavior may be attributed to the fact that the decrease in settlement improvement ratio to about (q/c_u) equals 1.48 to 2.8 associated by the increase in bearing ratio and beyond these values, the excess bulging leads to decrease in load carrying capacity. Also the lower improvement values (high degree of improvement) are observed when the embankment model is treated by ordinary stone columns at (s/d = 2.5) compared with the model at (s/d= 4) that revealed a high value of settlement improvement ratio for different heights of embankment. Settlement improvement ratio at failure is summarized in **Table 6**. The results are in agreement with the results of Craig and **Al-Kahafaji 1997, Rahil, 2007, Al-Waily, 2008, and Fattah et al. ,2011.**

Stress on column versus settlement: The vertical effective stress on column was measured at the top of the middle stone column under the center line of embankment and on the edge stone column using earth pressure cell for all models. The stress-settlement behavior of the stone columns for all spacing ratios is the same as shown in **Figs. 24 to 26**. The bearing capacity of the stone columns at failure

corresponding to settlement ratio of 10% increases with decreasing spacing distance between the columns, as shown in **Table 7**. These results agree with **Hewlett** and **Randolph, 1988, Low et al., 1994, Chen et al., 2007, Britton and Naughton, 2008 and Ellis and Aslam, 2009,** who measured the stress using different experimental models for piled embnkment.

The highest vertical effective stress is obtained in case of the least spacing (s/d = 2.5) is used under the embankment of height 300 mm. This phenomenon is due to the stress concentration occurring between the adjacent columns as well as due to the confinement effect provided by the surrounding soil and the adjacent stone columns therefore, the stress concentration on the stone columns increases with decreasing the spacing of columns. The decrease in vertical effective stress on the stone column as the spacing increases is due to the yielding of the stone column. Once yielded, the stiffness of the column decreases, its radial deformability increases due to dilitancy. Otherwise, the yielding of the column reduces the transfer of vertical load from the soil.

Stress on soft soil versus settlement: The vertical effective stress (σ'_{vc}) in reinforced soft soil was measured at the base of embankment between two columns using earth pressure cells. The relationship of the vertical effective stress with surface settlement of embankment is shown in **Figs. 27 to 29**. The vertical effective stress in the reinforced soft soil increases at a high rate with increasing spacing between stone columns and decreasing embankment fill height. This may be due to the excess bulging that occurs in the stone column which leads to decrease in load carrying capacity. Directly after the embankment construction stages have been finished, the vertical stress in the reinforced soft soil increases at a very small rate, and as stone columns spacing decreases, the vertical stress in the reinforced soil decreases and high stress values are generated in the stone column. This is due to the stress transfer from the soft soil and concentration of the stress in the stone column (soil arching phenomenon). **Table 8** summarizes the values of vertical effective stress on soft soil at failure corresponding to settlement ratio of 10%. These results agree with **Hewlett** and **Randolph, 1988, Low et al., 1994, Chen et al., 2008, Britton and Naughton, 2008, and Ellis and Aslam, 2009,** who measured the stress using different experimental models for piled embankment.

5. CONCLUSIONS

The following points are drawn from the test results:

1. The mode of failure for embankment model resting on untreated very soft clay with cu ≈ 10 kPa is close to local shear failure and the mode gradually changes toward the general shear with using stone columns.
2. The bearing ratio increases with decreasing spacing distance between the stone columns at any embankment height. The rate of increasing in bearing ratio of treated models was found to be within the range (1.08 to 1.2); (1.23 to 1.42) and (1.37 to 1.65) of untreated models for embankment model height of 200 mm, 250 mm and 300 mm, respectively.

3. The bearing improvement ratio increases with decreasing spacing ratio of stone column for given embankment. Higher improvement ratio was achieved for the models treated with stone columns at S=2.5d at any embankment high. The higher values of (q_t / q_{unt}) was found to be (1.21, 1.44 and 1.7) for embankment model of height 200 mm, 250 mm and 300 mm, respectively while lowest improvement was observed at spacing s = 4d especially for embankment height 200 mm.

4. The improvement in settlement ratio increases as the spacing ratio of stone columns increases. The lowest value of settlement improvement ratio at failure was observed at s=2.5d for a given embankment height, which represents higher degree of improvement.

6. REFERENCES

Al-Mosawe, M.J., Abbass, A.J. and Majeed, A.H. ,1985, *Prediction of Ultimate Capacity of a Single and Groups of Stone Columns*, Iraqi Conference on Engineering ICE 85, Vol.1, Baghdad.

Al-Qayssi, M.R. ,2001, *Unreinforced and Reinforced Behavior of Single and Groups of Granular Piles,* Ph.D. Thesis, Civil Engineering Department, Faculty of the Military College of Engineering, Iraq.

Al-Shaikhly, A.A. 2000, *Effect of Stone Grain Size on the Behavior of Stone Column*, M.Sc. Thesis, Building and Construction Engineering Department, University of Technology, Iraq.

Al-Waily, M. J. , 2008, *Stress Concentration Ratio of Model Stone Columns Improved by Additives*, Ph.D. Thesis, Building and Construction Engineering Department, University of Technology, Iraq.

ASTM, D422 2003, *Standard Test Method for Particle-Size Analysis of Soils* Soil and Rock (I), Vol. 04.08.

ASTM, D854 2003, *Standard Test Method for Specific Gravity of Soil Solids by Water Pycnometer*, Soil and Rock (I), Vol. 04.08.

ASTM, D4318 ,2003, *Standard Test Method for Liquid Limit, Plastic Limit, and Plasticity Index of Soils*, Soil and Rock (I), Vol. 04.08.

British Standard B.S.:1377 part 2 ,1990, *Methods of Test for Soils for Civil Engineering Purposes General Requirements and Sample Preparation*, British Standard Institution, London.

Britton, E. and Naughton, P. ,2008, *An Experimental Investigation of Arching in Piled Embankments*, Proceedings of the 4th European Geosynthetics Conference, Edinburgh, UK, September 2008, No. 106, pp. 1-8

Chen, Y.M., Cao, W.P. and Chen, R.P. , 2007, *An Experimental Investigation of Soil Arching within Basal Reinforced and Unreinforced Piled Embankments* Geotextiles and Geomembranes, Vol. 26, pp. 164-174.

Cragi, W.H. and Al-Khafaji, Z.A. , 1997, *Reduction of Soft Clay Settlement by Compacted Sand Piles*, Proceeding of the 3rd International Conference of Ground Improvement, London, pp.218-224.

Chen, R.P., Chen, Y.M., Han, J. and Xu, Z.Z. 2008, *A Theoretical Solution for Pile – Supported Embankments on Soft Soils under One Dimensional Compression*, Canadian Geotechnical Journal, Vol. 45, No. 5, pp. 611-623.

Ellis, E.A. and Aslam, R. , 2009, *Arching in Piled Embankments: Comparison of Centrifuge Tests and Predictive Methods* – Part 1 of 2. Ground Engineering, pp. 34-38.

Fattah, M. Y, Shlash, K. T., and Al-Waily, M.J. 2011, *Stress Concentration Ratio of Model Stone Columns in Soft Clays*, Geotechnical Testing Journal, Vol. 34, No. 1, pp. 61-71.

Han, J. and Gabr, M.A. 2002, *Numerical Analysis of Geosynthetic Reinforced and Pile-Supported Earth Platforms over Soft Soil*, Journal of Geotechnical and Geoenvironmental Engineering, pp. 44-53.

1Hewlett, W.J. and Randolph, M.F. 1988, *Analysis of Piled Embankments*, Ground Engineering, Vol. 21, No. 3, pp. 12-18.

Hughes, J.M.O. and Withers, N.J. 1974, *Reinforcing of Soft Cohesive Soils with Stone Columns*, Ground Engineering Journal, Vol. 7, No. 3, pp. 42-49.
Juran, I. and Guermazi, A. 1988, *Settlement Response of Soft Soil Reinforced by Compacted Sand Columns*, Journal of Geotechnical Engineering, ASCE, Vol.114, No.8, pp.930-943.
Kempfert, H.G. ,2003, *Ground Improvement Methods with Special Emphasis on Column-Type Techniques*, Int. Workshop on Geotechnics of Soft Soils-Theory and Practice. Vermeer, Schweiger, Karstunen & Cudny (eds.).
Low, B.K., Tang, S.K. and Choa, V. ,1994, *Arching in Piled Embankments*, Journal of Geotechnical Engineering, ASCE, Vol. 120, No. 11, pp. 1917-1938.
Madhav, M.R., Alamgir, M. and Miura, N. 1994, *Improving Granular Column Capacity by Geogrid Reinforcement*, Proceedings of the 5th International Conference on Geotextiles, Geomembranes and Related Products, Vol. 1, Singapore, pp. 351-356.
Murugesan, S. and Rajagopal, K. 2006, *Geosynthetic-Encased Stone Columns: Numerical Evaluation*, Geotextiles and Geomembranes, Vol. 24, No.6, pp. 349–358.
Rahil, F.H. 2007, *Improvement of Soft Clay Underneath a Railway Track Model using Stone Columns Technique*, Ph.D. Thesis, Building and Construction Engineering Department, University of Technology, Iraq.
Rao, S.N., Reddy, K.M. and Kummar, P.H. ,1997, *Studies on Group of Stone Columns in Soft Clays.*, Journal of Geotechnical Engineering, Southeast Asian, Vol. 28, No. 2, Dec., pp.165-181.
Yoo C. 2010, *Performance of Geosynthetic-Encased Stone Columns in Embankment Construction: Numerical Investigation*, Journal of Geotechnical and Geoenvironmental Engineering, ASCE, Vol. 136, No. 8, pp. 1148-1160.

Table 1. Physical and chemical properties of natural soil used.

Property	Value
Liquid limit (LL) %	47
Plastic limit (PL) %	23
Plasticity index (PI) %	24
Specific gravity (G_s)	2.7
% Passing sieve No. 200	94
Sand content % (0.075 to 4.75 mm)	6
Silt content % (0.005 to 0.075 mm)	48
Clay content % (< 0.005 mm)	46
Maximum dry unit weight (kN/m^3)	18.24
Optimum moisture content (%)	13
Soil symbol according to USCS	CL
Total soluble salts (%)	6.13
SO_3 (%)	0.6
Organic matter (%)	1.09
Gypsum content (%)	1.17
pH	8.34

Table 2: Physical properties of the crushed stone.

Property	Value
Maximum dry unit weight (kN/m^3)	15.7
Minimum dry unit weight (kN/m^3)	13
Dry unit weight (kN/m^3) at	
Dr =55%	14.4
D_{10} (mm)	3.8
D_{30} (mm)	6
D_{60} (mm)	7.5
Coefficient of uniformity (C_u)	1.97
Coefficient of curvature (C_c)	1.26
Angle of internal friction ($Ø^o$)	41.5
Specific gravity (G_s)	2.65

Table 3: Physical and chemical properties of the sub-base material used.

Property	Value
CBR (%)	51
Maximum dry unit weight (kN/m^3)	21.84
Optimum moisture content (%)	6.3
D_{10} (mm)	0.15
D_{30} (mm)	1.5
D_{60} (mm)	12
Coefficient of uniformity (C_u)	80
Coefficient of curvature (C_c)	1.25
Angle of internal friction ($Ø^o$)	40
SO_3 (%)	0.23
Total soluble salts (%)	2.93
Gypsum content (%)	0.494
Organic matter (%)	0.057

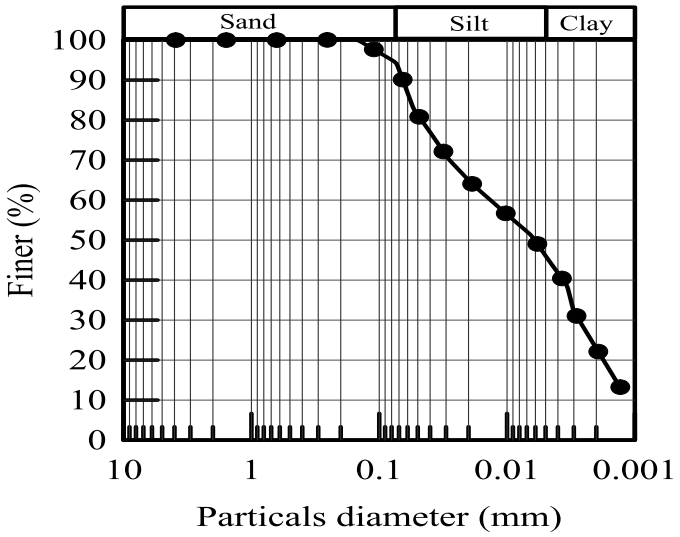

Figure 1. Grain size distribution of clayey soil used.

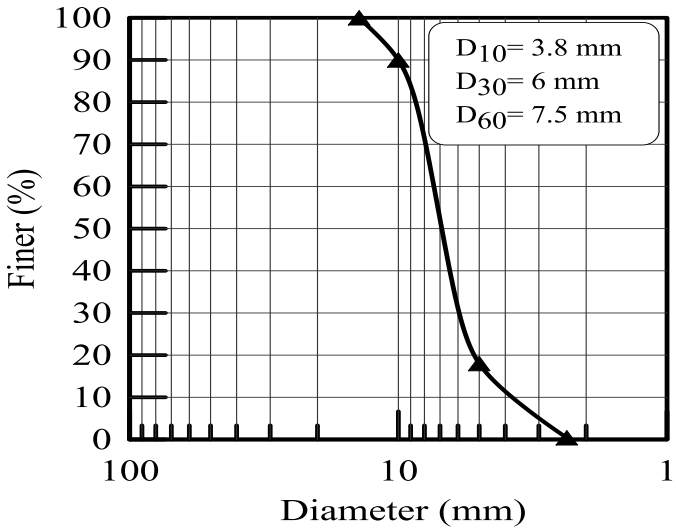

Figure 2. Grain size distribution of stone used.

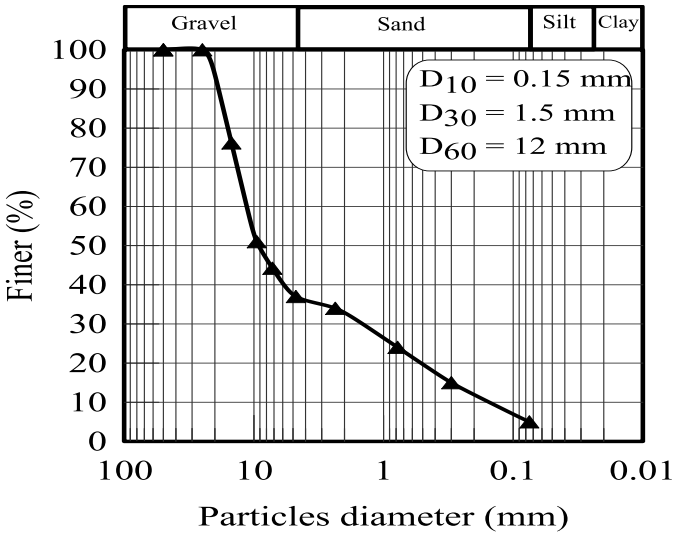

Figure 3. Grain size distribution sub-base material used.

Plate 1. Experimental test container and loading system.

Plate 2. Load cell and load readout.

Plate 3. Earth pressure cell model 4800.

Plate 4. Readout of pressure cell.

Plate 5. Portable vane shear device.

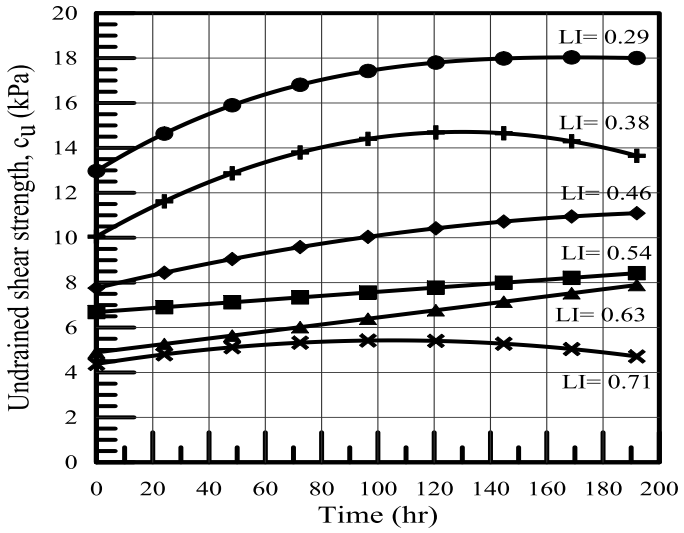

Figure 4. Variation of undrained shear strength with time after mixing.

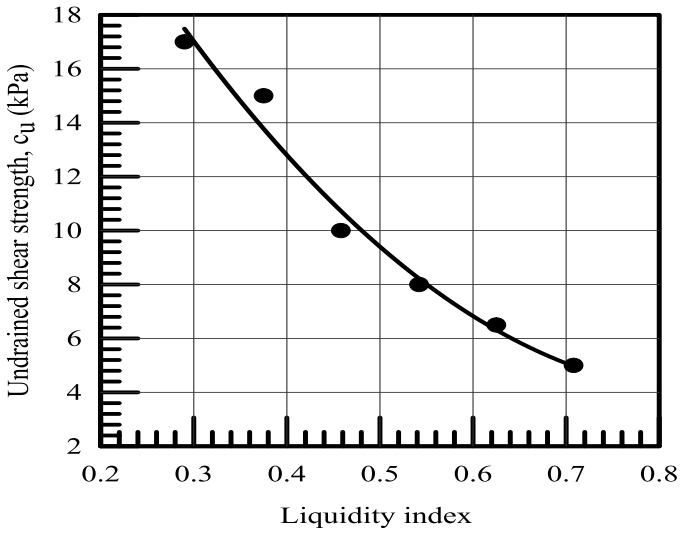

Figure 5. Variation of the undraied shear strength with liquidity index.

Plate 6. Soil preparation inside the manufactured container.

Plate 7. The process of stone column installation.

Plate 8. Configuration of patterns of stone columns, S= 3d.

Plate 9. Installation of embankment fill.

Plate 10. Model testing procedure.

Plate 11. Stone columns failure (S=3d, L/d=8).

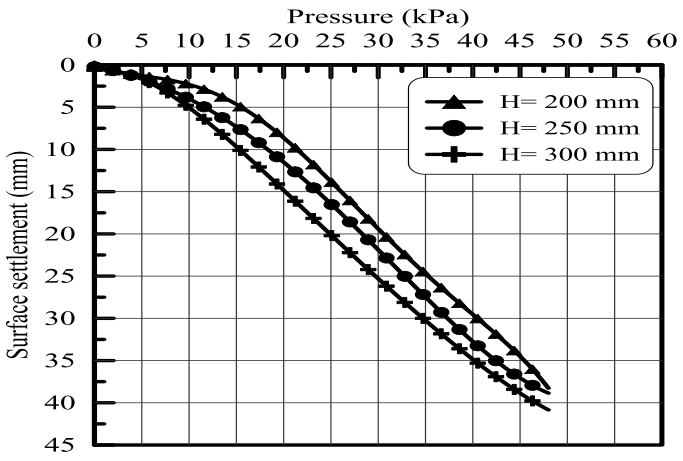

Figure 6. Bearing pressure versus surface settlement for untreated embankment model.

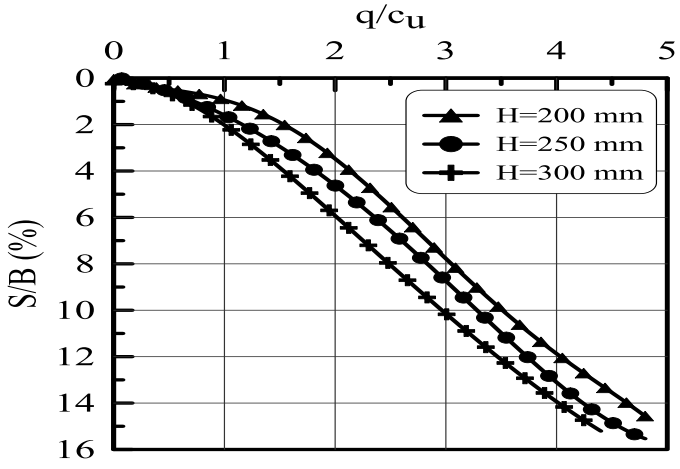

Figure 7. Bearing ratio versus settlement ratio for untreated embankment model.

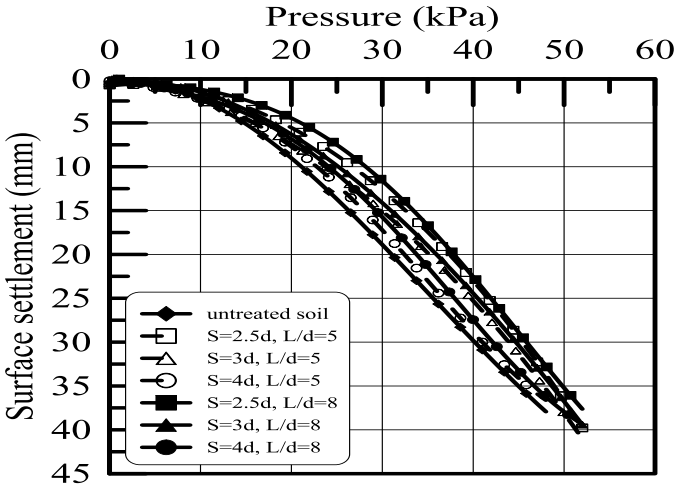

Figure 8. Bearing pressure versus settlement for embankment model 200 mm high resting on soft soil treated by stone columns.

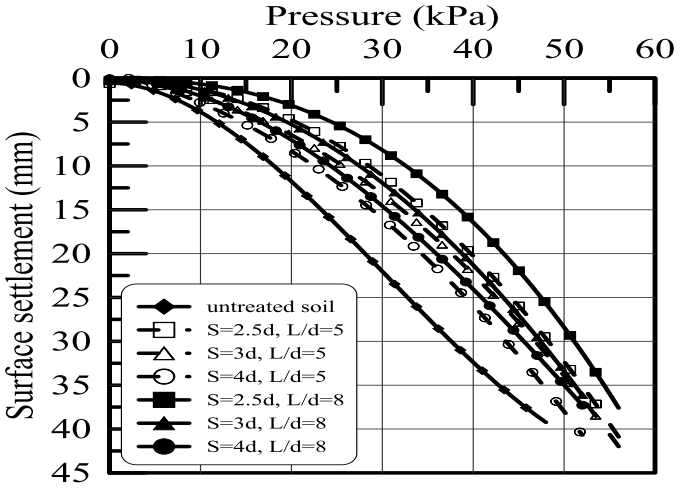

Figure 9. Bearing pressure versus settlement for embankment model 250 mm high resting on soft soil treated by stone columns.

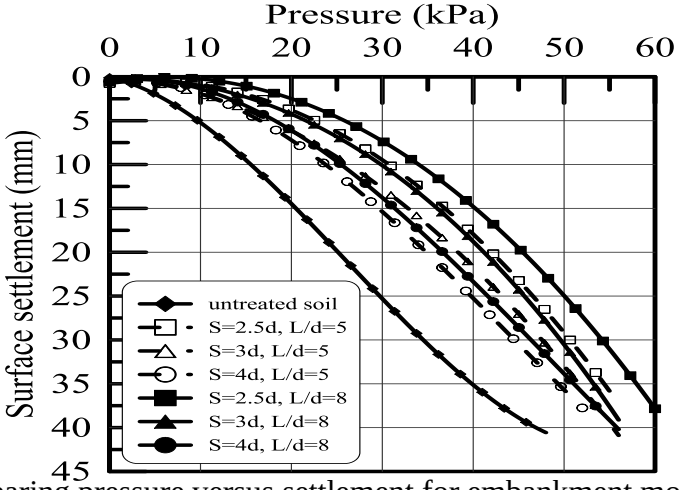

Figure 10: Bearing pressure versus settlement for embankment model 300 mm high resting on soft soil treated by stone columns.

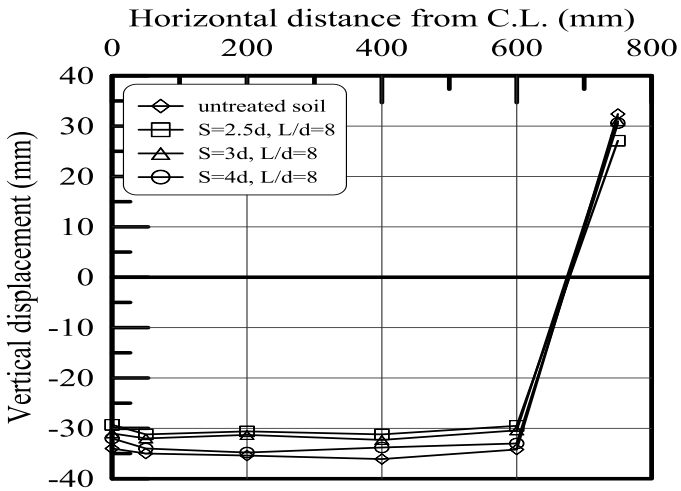

Figure 11. Settlement distribution at the base of embankment model 200 mm high constructed on soft soil treated by stone columns and L/d = 8.

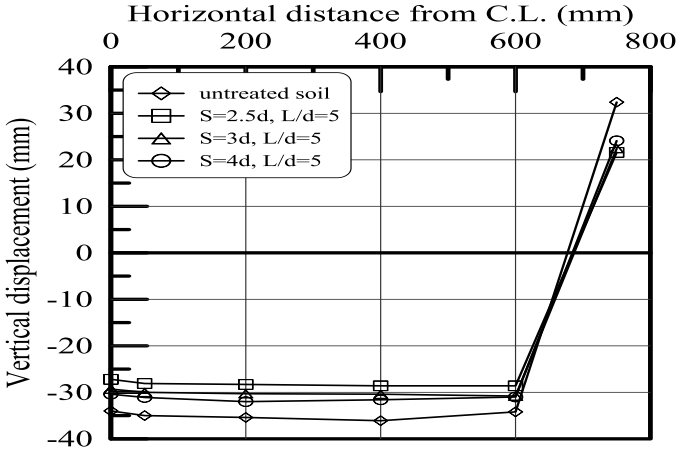

Figures 12. Settlement distribution at the base of embankment model 200 mm high constructed on soft soil treated by stone columns and L/d = 5.

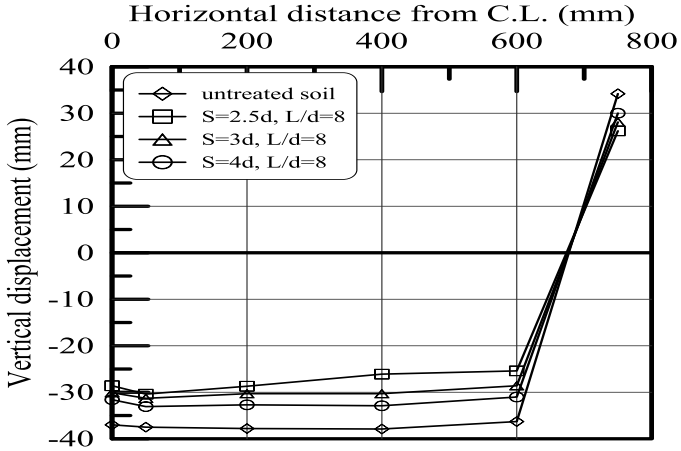

Figures 13. Settlement distribution at the base of embankment model 300 mm high constructed on soft soil treated by stone columns and L/d = 8.

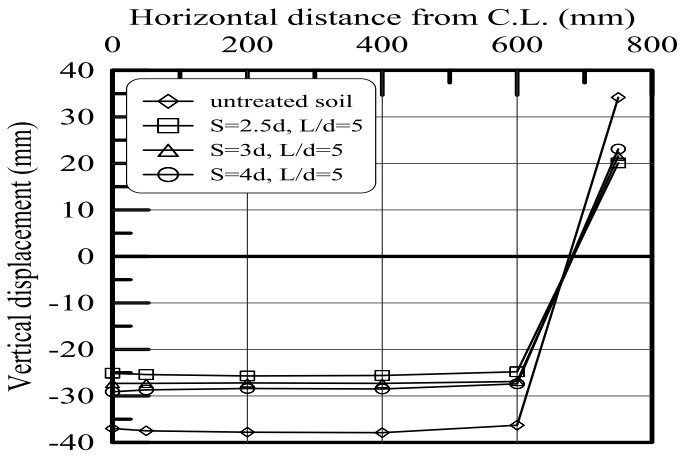

Figures 14. Settlement distribution at the base of embankment model 300 mm high constructed on soft soil treated by stone columns (OSC) and L/d = 5.

Table 4. Bearing ratio at failure for embankment model constructed on soft clay treated by stone columns.

Spacing	Bearing ratio, q/c_u					
	H=200 mm		H=250 mm		H=300 mm	
L/d ratio	5	8	5	8	5	8
Untreated soil	3.5		3.3		3.0	
S= 2.5d	4.1	4.2	4.3	4.7	4.6	5.0
S= 3d	3.9	4.0	4.2	4.3	4.3	4.5
S= 4d	3.65	3.8	3.8	4.05	4.0	4.1

Table 5. Bearing improvement ratio at failure for embankment models constructed on soft clay treated by stone columns.

Spacing	Bearing improvement ratio, q_t/q_{unt}					
	H=200 mm		H=250 mm		H=300 mm	
L/d ratio	5	8	5	8	5	8
S= 2.5d	1.2	1.21	1.38	1.43	1.63	1.7
S= 3d	1.11	1.15	1.30	1.36	1.42	1.55
S= 4d	1.06	1.09	1.20	1.23	1.35	1.43

Table 6. Settlement improvement ratio at failure for embankment models constructed on soft clay treated by stone columns.

Spacing	Settlement improvement ratio, S_t/S_{unt}					
	H=200 mm		H=250 mm		H=300 mm	
L/d ratio	5	8	5	8	5	8
S= 2.5d	0.88	0.78	0.72	0.67	0.61	0.56
S= 3d	0.89	0.81	0.78	0.70	0.70	0.62
S= 4d	0.96	0.91	0.88	0.72	0.74	0.70

Table 7. Vertical effective stress on stone column at failure for embankment models constructed on soft clay treated by 7stone columns.

Spacing	Stress on column (kPa)					
	H=200 mm		H=250 mm		H=300 mm	
L/d	5	8	5	8	5	8
S= 2.5d	16	18.8	23.6	31	25	36
S= 3d	15	17	19.8	23.6	22.8	31
S= 4d	11.6	13.3	14.5	19.8	17.5	21

Table 8. Vertical effective stress in soil at failure for embankment models constructed on soft clay treated by stone columns.

Spacing	Stress in soil (kPa)					
	H=200 mm		H=250 mm		H=300 mm	
L/d	5	8	5	8	5	8
S= 2.5d	23	22.5	19.8	18	18.3	16.2
S= 3d	27.2	26.5	24.8	23.9	22	20.5
S= 4d	30.5	27.5	27	25.8	24.6	23

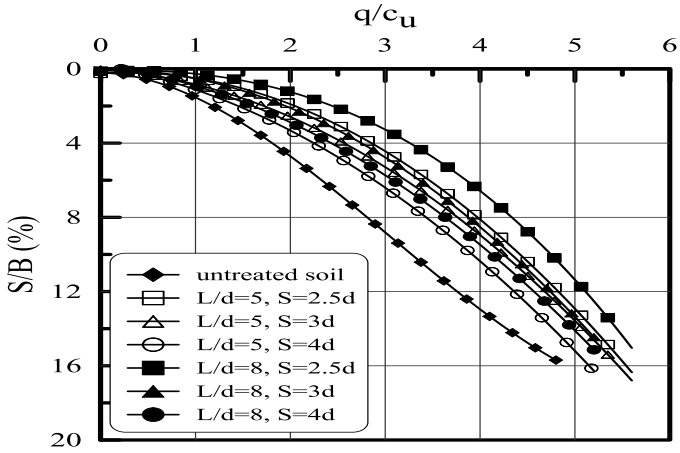

Figure 15. Bearing ratio versus settlement ratio for embankment model 200 mm high resting on soft soil treated by stone columns.

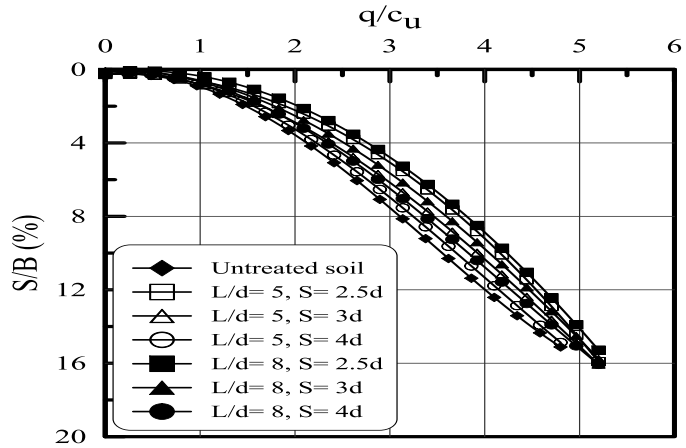

Figure 16. Bearing ratio versus settlement ratio for embankment model 250 mm high resting on soft soil treated by stone columns.

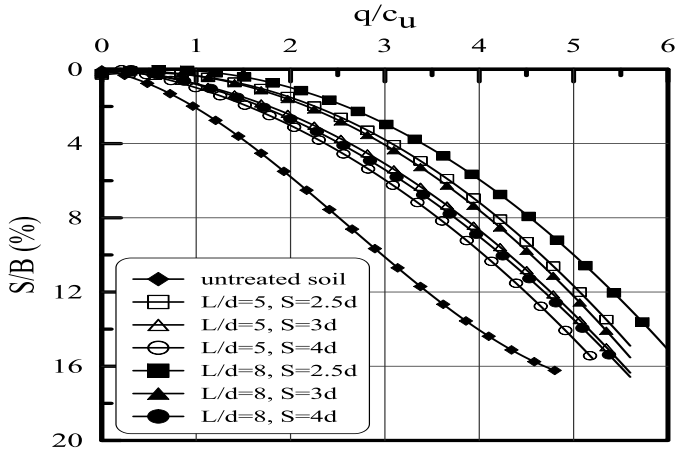

Figure 17. Bearing ratio versus settlement ratio for embankment model 300 mm high resting on soft soil treated by stone columns.

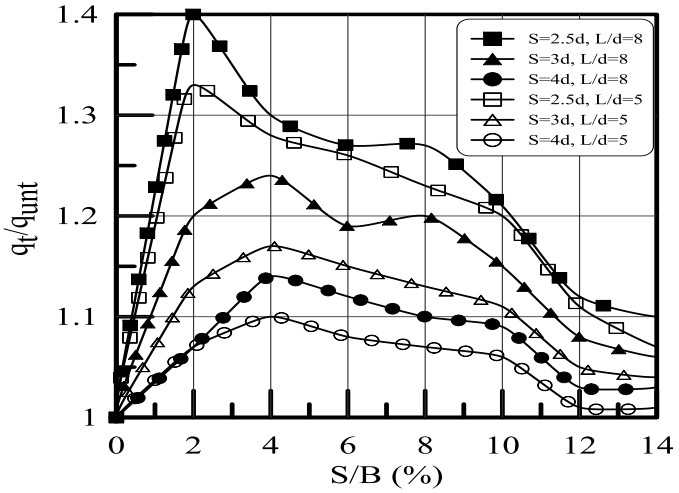

Figure 18. Bearing improvement ratio versus settlement ratio for embankment 200 mm high resting on soft soil treated by stone columns.

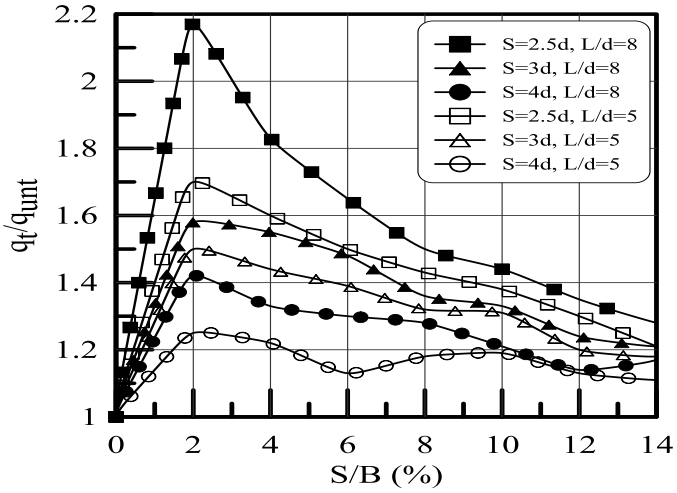

Figure 19. Bearing improvement ratio versus settlement ratio for embankment 250 mm high resting on soft soil treated by stone columns.

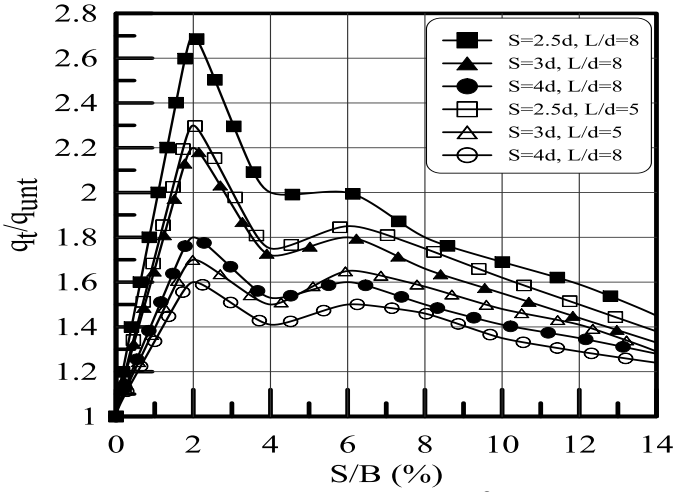

Figure 20. Bearing improvement ratio versus settlement ratio for embankment 300 mm high resting on soft soil treated by stone columns.

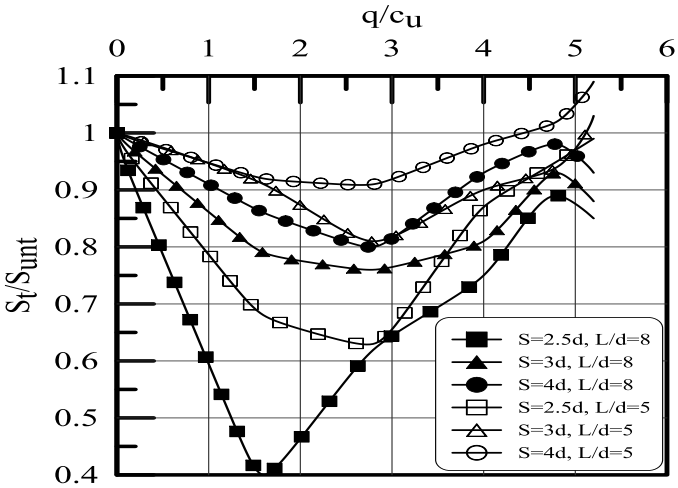

Figure 21. Settlement improvement ratio versus bearing ratio for embankment 200 mm high resting on soft soil treated by stone columns.

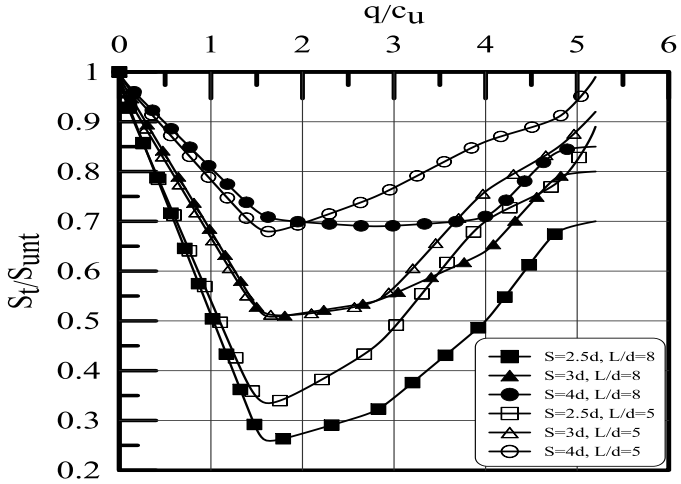

Figure 22. Settlement improvement ratio versus bearing ratio for embankment 250 mm high resting on soft soil treated by stone columns.

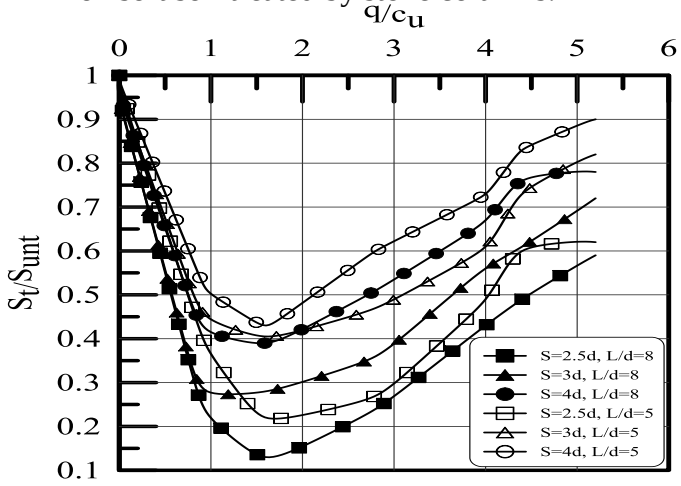

Figure 23. Settlement improvement ratio versus bearing ratio for embankment 300 mm high resting on soft soil treated by stone columns.

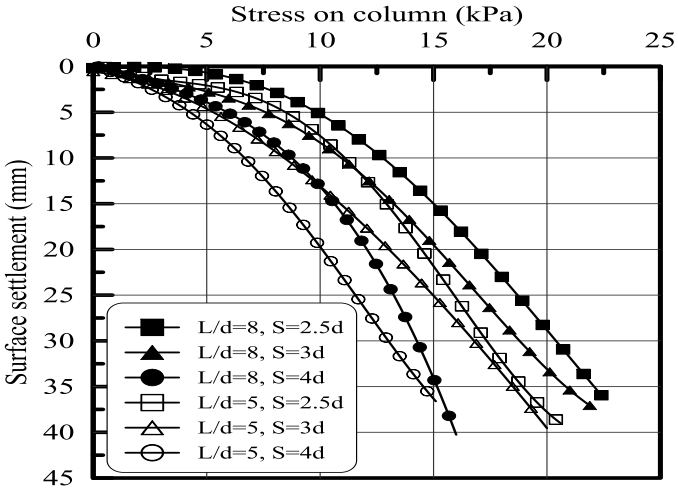

Figure 24. Vertical effective stress on column at failure versus surface settlement for embankment model of 200 mm height constructed on soft soil treated by stone columns.

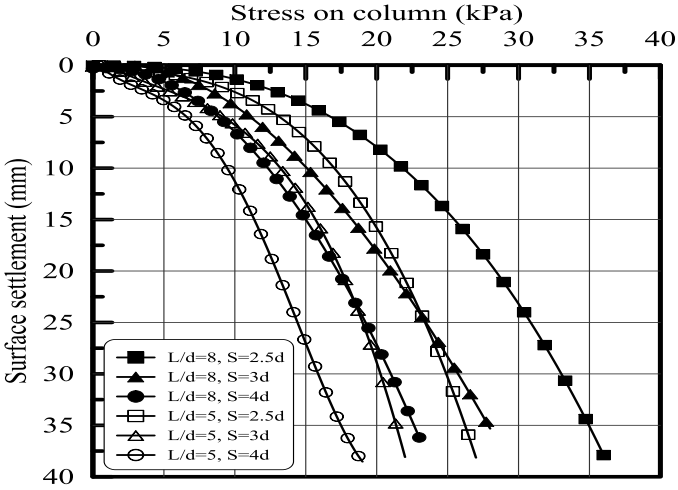

Figure 25. Vertical effective stress on column at failure versus surface settlement for embankment model of 250 mm height constructed on soft soil treated by stone columns.

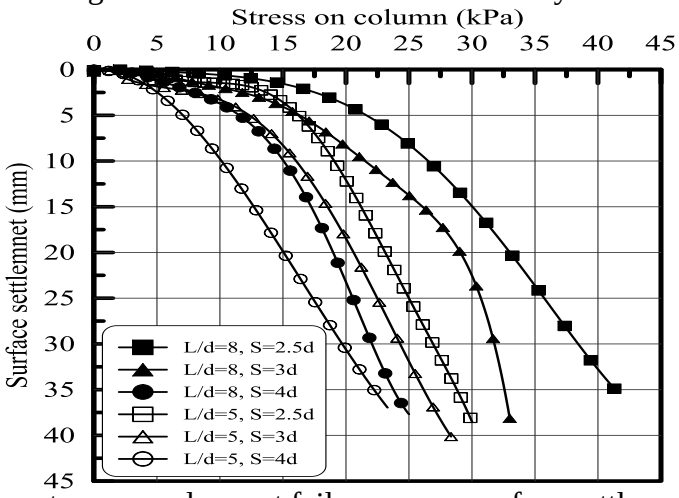

Figure 26. Vertical effective stress on column at failure versus surface settlement for embankment model of 300 mm height constructed on soft soil treated by stone columns.

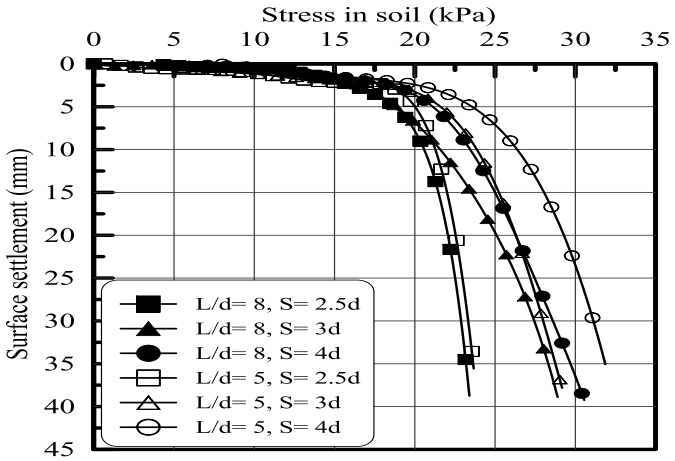

Figure 27. Vertical effective stress in soil at failure versus surface settlement for embankment model of 200 mm height constructed on soft soil treated by stone columns.

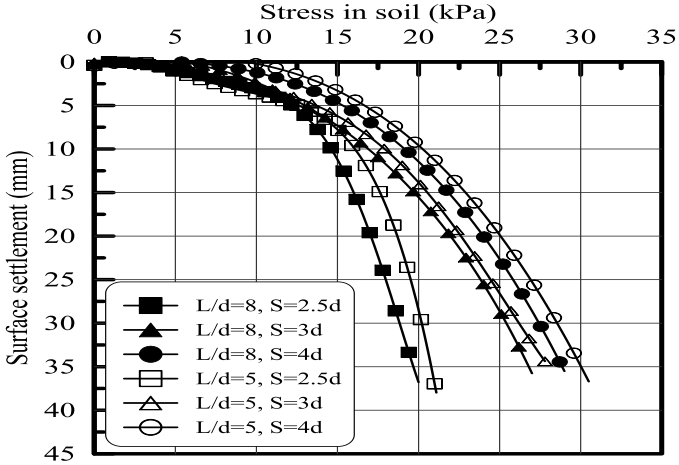

Figure 28. Vertical effective stress in soil at failure versus surface settlement for embankment model of 250 mm height constructed on soft soil treated by stone columns.

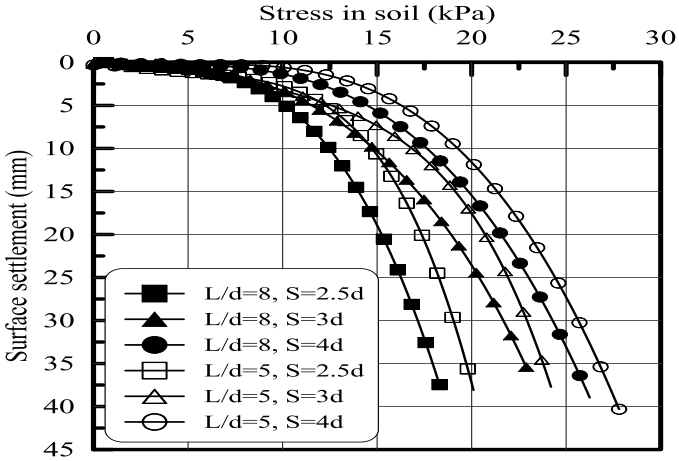

Figure 29. Vertical effective stress in soil at failure versus surface settlement for embankment model of 300 mm height constructed on soft soil treated by stone columns.